# SURFACE ROUGHNESS, CLUSTERING AND MATERIAL EFFECTS IN ABSORPTION AND SCATTERING BY ELECTRICALLY SMALL PARTICLES

Herschel Weil
Radiation Laboratory
Department of Electrical Engineering and Computer Science
The University of Michigan
Ann Arbor, Michigan 48109

RECENT PUBLICATIONS, SUBMITTALS FOR PUBLICATION AND PRESENTATIONS:

A) H. Weil, T.B.A. Senior, "Structure of Surface Polariton Modes in and Near Small Particles", presented to U.S. Nat. Comm. of URSI, Radio Science Meeting, Boulder, CO, January 1984.
B) T.B.A. Senior and D. A. Ksienski, "Determination of a Vector Potential", Radio Sci., 19, pp. 603-607, March-April 1984.
C) T.B.A. Senior and M. Naor, "Low Frequency Scattering by a Resistive Plate", IEEE Trans. Antennas and Propagat., Vol. AP-21, pp. 272-275, March 1984.
D) D. A. Ksienski, "Scattering by Distributions of Small Particles", Ph.D. Dissertation, University of Michigan, December 1984.
E) H. Weil, "Transmission and Absorption of Radiation in Particle Clouds,", Final Report on CSL Contract DAAK11-82-K-0007, May 1985.
F) H. Weil, T.B.A. Senior and T. M. Willis III, "Internal and Near Fields of Small Particles Irradiated in Spectral Absorption Bands", J. Opt. Soc. Amer. A, Vol. 2, pp. 989-996, June 1985.
G) H. Weil and T.B.A. Senior, "Absorption and Scattering by Small Particles; Structure of Internal and Near Fields", Proc. 1984 CSL Conference on Obscuration and Aerosol Research, pp. 295-296, June 1985.
H) T.B.A. Senior and D. A. Ksienski, "Low Frequency Scattering by Dielectric Platelets", Applied Physics B (to appear) Vol. 38, pp. 3160-3166 (provisional page numbers), 1985.

## ABSTRACT

Resonance absorption and scattering by polariton modes for Rayleigh particles and particle clusters are studied numerically. The effects on the resonance frequencies and resonance strengths of particle shape and contiguity and of surface grooves and ridges are illustrated for a number of particle configurations.

## INTRODUCTION

The resonances we are concerned with occur in absorption bands of the bulk material of which the particles are composed. The absorption is due to combined electromagnetic-vibrational modes of excitation; i.e., polariton modes. The resonances occur even in particles which are much smaller than the wavelength of the purely electromagnetic incident wave, so-called Rayleigh particles. Since the results we present are all based on the theory, computational techniques and computer programs presented in Refs. A), E), F) and G) listed above as well as in an older related paper [Senior and Weil, Appl. Phys. B 29, 117, 1982]; we simply quote without proof the theoretical formulas essential to understand the significance of the present results. A requirement on the applicability of the results is that the entire group of one or more scatterers must lie within a region small compared to the free space wavelength. We shall consider such a group of particles to be a single disjoint scatterer. To simplify the problem while still retaining the effects we wish to demonstrate we assume that all the scatterers are rotationally symmetric about an axis which we take to be the $x_3$ axis of a Cartesian or cylindrical system. The polarization tensor, $\bar{\bar{X}}$, which relates the

unperturbed incident electric field $\bar{E}_0$ to the dipole moment of the induced field via

$$\bar{p} = \varepsilon_0 V \bar{\bar{X}} \bar{E}_0$$

then has a diagonal matrix with $X_{11} = X_{22}$. Element $X_{11}$ is proportional to the dipole moment when $\bar{E}_0$ is transverse to the symmetry axis, $X_{33}$ to the dipole moment, when $\bar{E}_0$ is parallel to the symmetry axis. $X_{11}$ and $X_{33}$ are functions of the complex dielectric constant $\varepsilon = \varepsilon' + i\varepsilon''$ of the bulk material composing the scatterer(s) (which are assumed to be homogeneous and nonmagnetic) and of their geometrical configuration. The absorption and total scattering cross-section $\sigma_A$ and $\sigma_T$ are expressible in terms of the $X_{ii}$. Thus if one averages over all orientations of the scatterer, considering all orientations to be equally likely the resulting average cross sections are

$$\langle\sigma_T\rangle = \frac{k_0^4 V^2}{18\pi} (2|X_{11}|^2 + |X_{33}|^2)$$

$$\langle\sigma_A\rangle = \frac{k_0 V}{3} \mathrm{Im}(2X_{11} + X_{33})$$

At the polariton resonances of $X_{11}$ or $X_{33}$ both absorption and scattering are enhanced.

The absorption bands of the bulk materials are characterized by a range of frequencies wherein $\varepsilon' < 0$ ($\varepsilon'' > 0$ always). The particle resonances occur for $\varepsilon' < 0$ and their strength depends on $\varepsilon''$. If $\varepsilon'' \equiv 0$, there is no damping and Im $X_i$ and $|X_{ii}|$ are infinite. Our procedures locate the important resonance values of $\varepsilon'$ by searching for those values which give clear maxima of Im $X_{ii}$ as a function of $\varepsilon'$ while $\varepsilon''$ is held fixed (independent of $\varepsilon'$)at a non-zero value small enough so as to avoid excessive damping. Of course for physically real materials $\varepsilon'$ and $\varepsilon''$ are both frequency dependent, $\varepsilon''$ varies with $\varepsilon'$. This is illustrated for Cu and SiC in Fig. 1 which plots $\varepsilon''$ vs $\varepsilon'$ for these materials while showing values of wavelength along the curve for Cu or normalized frequency $\nu$ = f/23.8 THz along the curve for SiC. We shall use these data to bring into account realistic material effects.

A good object with which to illustrate the resonance effects is the isolated sphere for which a simple formula exists for $X_{ii}$:

$$X_{11} = X_{33} = 3(\varepsilon - 1)/(\varepsilon + 2) \quad .$$

Hence there is one true resonance and this is for $\varepsilon' = -2$, $\varepsilon'' = 0$. To explore the effect of non-zero $\varepsilon''$ one can write

$$\varepsilon = -2 + \Delta + i\varepsilon''$$

so that

$$\text{Im } X_{11} = \text{Im } X_{33} = \frac{9\varepsilon''}{\Delta^2 + \varepsilon''^2}$$

which at resonance ($\Delta = 0$) shows that

$$\text{Im } X_{11} = 9/\varepsilon'' \ .$$

## RESULTS

### 1. Pairs of Spheres and Partial Spheres

We first consider the sequence of bodies shown in Fig. 2. This begins with a single sphere and then follows a sequence as though two superimposed spheres were being pulled apart, finally becoming a pair of separate spheres. For each configuration Fig. 2 also shows the location on the $-\varepsilon'$ axis of the resonances which are not damped out when $\varepsilon'' = 0.01$. Resonances for both $X_{11}$ and $X_{33}$ are shown. $X_{33}$ tends to have a larger number of appreciable resonances than $X_{11}$. There is also a sudden shift to an extremely large value of $-\varepsilon'$ for one of the $X_{33}$ resonances occurs just as the two spheres separate.

Next, to illustrate the relative peak strengths and resonance widths of the various resonances we plot $-\varepsilon'$ vs Im $X_{11}$ in Fig. 3 for one of the configurations in Fig. 3. We do this for the three materials; the unphysical one in which $\varepsilon'' = 0.01$ for all $\varepsilon'$, and for Cu and SiC. One might think of the resonances obtained for $\varepsilon'' = 0.01$ as putative resonances which may or may not be damped out by the $\varepsilon''$ values of a true material. We see that most, but not all, such potential resonances are in fact removed by damping for Cu and SiC.

### 2. Circular Disks and Pairs of Circular Disks

Results similar to those of Fig. 3 are given in Fig. 4 for a sequence made by "pulling apart" two superposed disks until they become separate pairs. The results are in some ways similar to those of spheres but note that a single disk, unlike a single sphere, possesses many potential resonances.

### 3. Surface Perturbations

In this section we illustrate how small scale perturbations of the surface can modify the strengths of the resonances as well as the $\varepsilon'$ values at which they occur. The perturbations also introduce new resonances. As a prototype unperturbed shape we use a spherically capped circular cylinder of five to one length to diameter ratio. Again we show the $X_{11}$ and $X_{33}$ resonances for the unphysical ($\varepsilon'' = 0.01$) material and for Cu and SiC. In Fig. 5(a) the $X_{11}$ results are shown for the unperturbed cylinder while Fig. 5(b) displays the results for surface modified as illustrated

with alternate ridges and grooves. Additional potential resonances are generated by the perturbations. Some, but not all, of these are suppressed by damping in the real materials. Figures 6(a) and 6(b) present similar results for $X_{33}$ and point up again that the number of resonances for $X_{33}$ is greater than for $X_{11}$.

## COMMENTS

Matrix elements $X_{11}$ and $X_{33}$ were each computed numerically from an integral equation based on the unperturbed field being respectively radially or axially directed. The limitation to rotational symmetry not only limited the matrix to only two non-zero elements it enabled analytic reduction of the integrals from surface to line integrals before any numerical procedure had to be introduced. When the particle is not rotationally symmetric the same type of diagonal matrix still exists for mirror symmetry of the body shape in the $x_1 x_3$ and $x_2 x_3$ planes.

Finally, we mention that Refs. D and H describe a completely different technique to handle thin disks of arbitrary shape. The method is a finite element one and gives identical results when applied to thin circular Rayleigh disks, as the integral equation mode used here, but it is not applicable in the polariton resonance regions without further refinement.

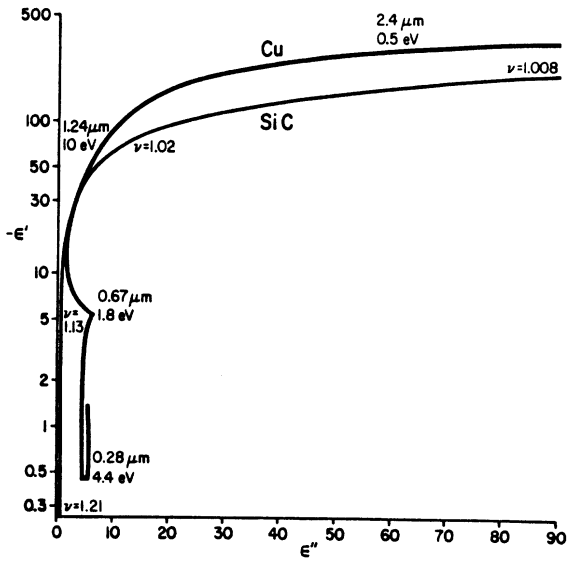



Fig. 1: The relationship ε" (ε') for Cu and SiC; wavelength or frequency as parameter. Data for Cu from Physik Daten; Part II, Fachinformationzentrum Energie, Physik, Mathematik, GMBH, Karlsruhe, 1981. Data for SiC from W. G. Spitzer, D. Kleinman and D. Walsh, Phys. Rev. 113, 127, January 1, 1959.

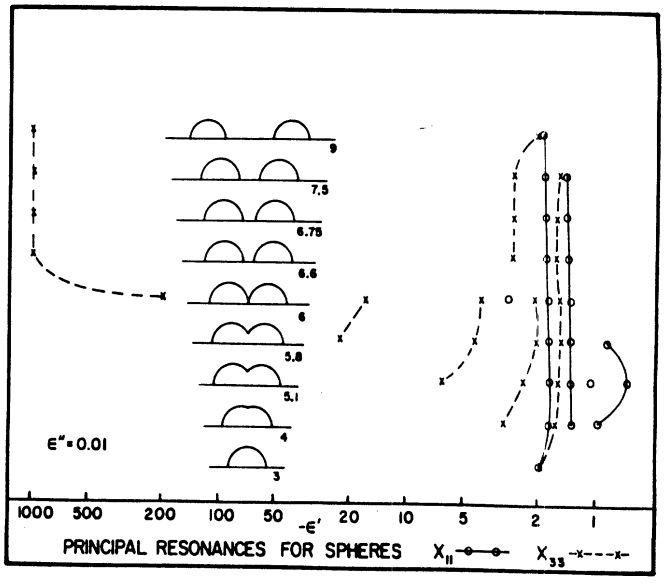



Fig. 2: Sphere sequence and associated principal resonance values of -ε' for both radial ($X_{11}$) and axial ($X_{33}$) $\bar{E}$ excitations.

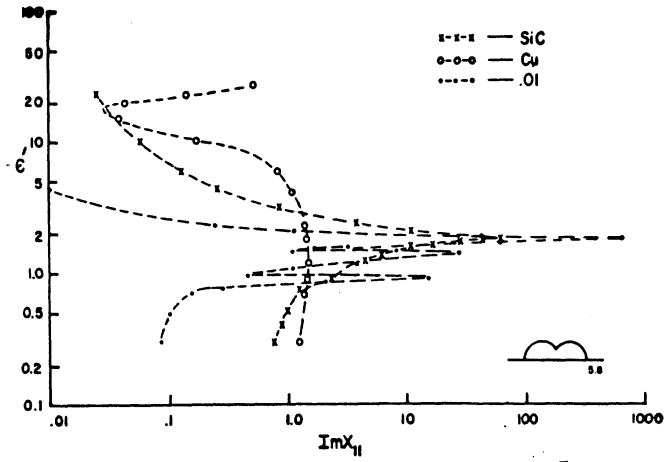



Fig. 3: Resonance strength for transverse $\bar{E}$ excitation of the configuration shown in the insert. This figure illustrates the damping effects of real materials Cu and SiC compared to the $\varepsilon' = 0.01$ hypothetical low damping material.

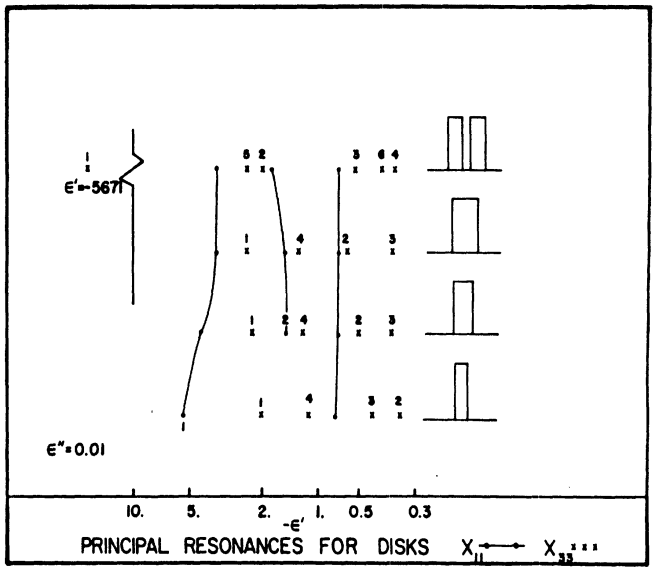



Fig. 4: Disk sequence and associated principal resonance values of $-\varepsilon'$ for both radial $X_{11}$ and axial $X_{33}$ $\bar{E}$ excitations.

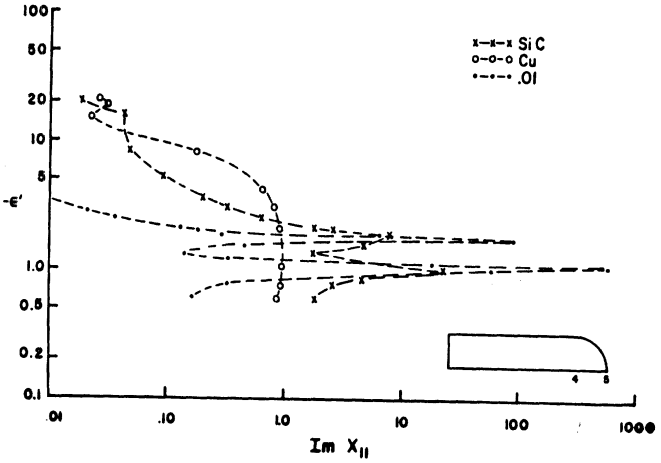



Fig. 5(a): Unperturbed surface.

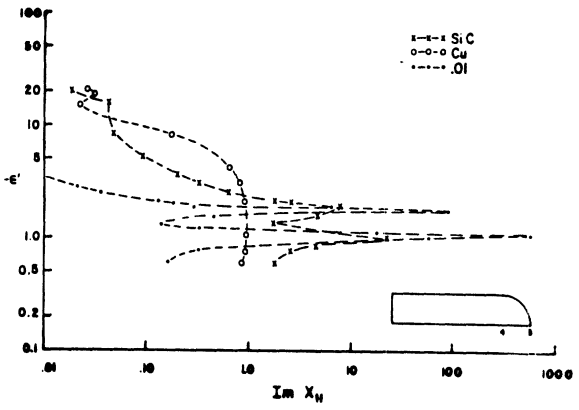



Fig. 5(b): With ridge and groove perturbations.

Resonance strengths for transverse excitation of a 5:1 hemispherically capped cylinder illustrating real material damping effects and surface perturbation effects.

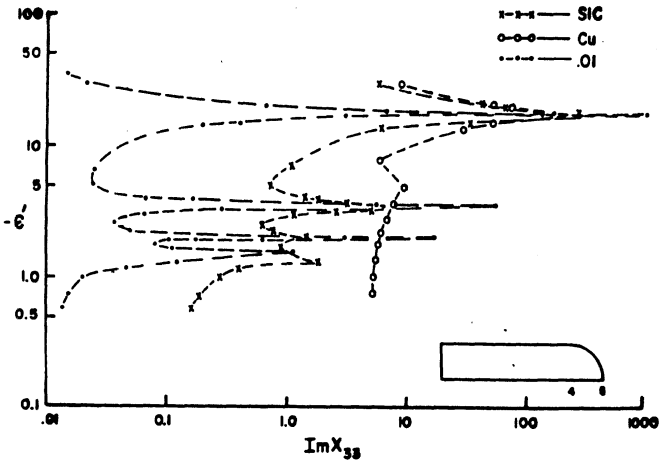



Fig. 6(a): Unperturbed surface.

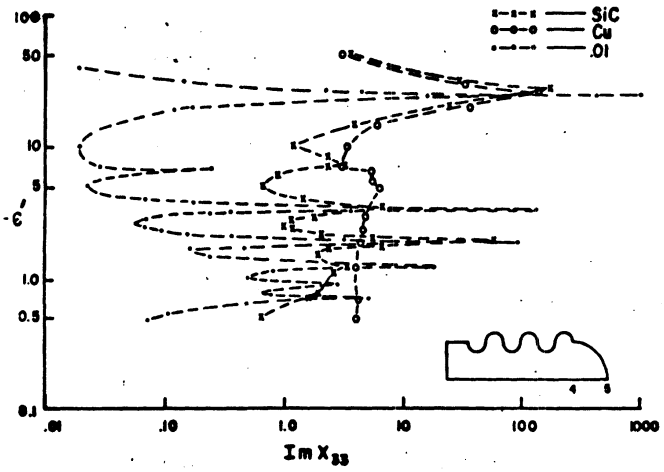



Fig. 6(b): With ridge and groove perturbations.

Resonance strengths for axial excitation of a 5:1 hemispherically capped cylinder illustrating real material damping effects and surface perturbation effects.